

A-1755

LPDR - (6)

WM-10(2); WM-11(2)

WM-16(2)

**Sandia National Laboratories**

Albuquerque, New Mexico 87185

PDR - (11)

January 15, ~~1986~~ <sup>1987</sup>

JAN 15 11:34

Mr. John Peshel  
Engineering Branch  
Division of Waste Management  
U.S. Nuclear Regulatory Commission  
7915 Eastern Avenue  
Silver Spring, MD 20910

Dear Mr. Peshel:

The enclosed monthly report summarizes the activities during the month of December for FIN A-1755.

If you have any questions, please feel free to contact me at FTS 844-8368 or L. R. Shipers at FTS 846-3051.

Sincerely,

*Robert M. Cranwell*

Robert M. Cranwell  
Supervisor  
Waste Management Systems  
Division 6431

RMC:6431

Enclosure

- Copy to:
- Office of the Director, NMSS
  - Attn: Program Support Branch
  - 6400 R. C. Cochrell
  - 6430 N. R. Ortiz
  - 6431 R. M. Cranwell
  - 6431 L. R. Shipers
  - 6431 K. K. Wahi
  - 6431 G. F. Wilkinson

8701230113 870115  
PDR WMRES EXISANL  
A-1755 PDR

WM-RES  
WM Record File  
A1755  
SNL

WM Project 10, 11, 16  
Docket No. \_\_\_\_\_

PDR ✓  
LPDR ✓ (B, N, S)

Distribution:

Peshel	Joan-ticket
(Return to WM, 623-SS)	Sac

3616

PROGRAM: Coupled Thermal-Hydrological- Mechanical Assessments and Site Characterization Activities for Geologic Repositories FIN#: A-1755

CONTRACTOR: Sandia National Laboratories BUDGET PERIOD: 10/86 - 9/87

DRA PROGRAM MANAGER: J. Peshel BUDGET AMOUNT: 250K

CONTRACT PROGRAM MANAGER: R. M. Cranwell FTS PHONE: 844-8368

PRINCIPAL INVESTIGATOR: L. R. Shippers FTS PHONE: 846-3051

#### PROJECT OBJECTIVES

To provide technical assistance to NRC in the assessment of coupled thermal-hydrological-mechanical phenomena and site characterization activities for high-level waste repositories.

#### ACTIVITIES DURING DECEMBER 1986

##### Activities and Accomplishments

A number of activities took place during the month of December for this project. The review and analysis of a "Computational Brief" authored by S. J. Mitchell was completed and is reported here. Attachment IA contains general and specific review comments on the document. Attachment IB describes the independent calculations done at SNLA to assess the adequacy of various analyses performed in the document. Good agreement is seen only when the same set of assumptions are made regarding thermal stresses. Significantly different results are obtained when proper account is made of the various excavation and thermal loads.

The STEALTH 2D model calculation of the horizontal cross-section of a shaft at BWIP was also completed and analyzed. The analysis and results are presented in Attachment II. Failure zones in the liner and grout are indicated. However, for the strength value and failure model that were used, no failure zones were observed in basalt.

The "Update" format conversions for the STEALTH 3D code were completed and a standard verification problem was run successfully. The steps necessary for the conversion to "Update" format are given in Attachment III. Due to a major change in the CRAY Operating System at Sandia, some difficulties are expected in the next two months. As a result, it may not be feasible to use large computer codes for some limited time.

A review of the BWIP document titled "Task V Engineering Study No.11 Shaft Casing Design Criteria and Methodology" was

initiated. Unless pre-empted by other NRC activities with a higher priority, this review will be completed in January, 1987.

Travel

None.

Problems Encountered

None.

ATTACHMENT IA

Subject: Document Review of a BWIP "Computational Brief" (Draft document)

Document Title: "Evaluation of Damaged Rock Zone Around Repository Openings"

Document Author: S. J. Mitchell

Issue Date: March 13, 1986

Reviewer: K. K. Wahi

General Comments

1. A preface to this document (included as p. iv) makes some statements and clarifications that are worth noting. The following points paraphrase important parts of the Errata contained in the preface.
  - The contents of this document will be published in summary form in a Supporting Document (SD). The SD will contain a more complete description of the analyses.
  - In the context of this document, the terms yield zone, progressive failure zone, plastic zone, and damaged rock zone are used synonymously. The term "yield zone" is considered as the most appropriate terminology for the phenomenon analyzed.
  - Part II of the Computational Brief (concerning fracturing induced by thermal expansion of vesicular fluid) neglected to note other work and alternative approaches available on the subject.
2. The sources of laboratory and field data have not been identified properly in several instances. Furthermore, intact values have been used as rock mass values in certain cases.
3. It appears that the numerical values chosen for various strength parameters are from the higher end of the range and, therefore, not representative or conservative.
4. The reviewer has performed his own analyses with different techniques. Whereas agreement exists in the predicted displacements and depth of damaged rock zone for given sets of applied loads and properties, the stress concentrations and thermal stresses assumed by Mitchell are thought to be too low. Calculations show that the stress levels around an emplacement hole are significantly higher when all excavation stresses and a proper thermal gradient are considered. Attachment I B includes a description and discussion of the analysis performed by the reviewer.
5. Two major weaknesses in the analytical approach used by Mitchell are:
  - 1) inability to account for a realistic temperature distribution and, hence, a thermal stress distribution;

- 2) excavation stresses of a room opening are not superimposed on excavation stresses for the emplacement hole.

### Specific Comments

- p. I.1 Thermally induced stresses have been incorporated by increasing the far-field stresses. The assumption of spatially uniform stress increase due to a constant temperature change fails to develop proper stress gradients or stress concentrations. It also tends to bring the in-situ stress ratio closer to unity. The net effect is a less severe loading scenario with respect to peak stress and regions of tensile stress near the opening. The addition of a constant thermal stress value to each component of stress also tends to increase the average stress or pressure. The yield strength of most rocks increases with pressure. The net effect is that yield strength may become artificially high away from the hot region. The approach used is, therefore, not conservative in determining proximity to yield (i.e., damaged rock zone) surface. The definition of disturbed zone as used is restrictive in that plastic yielding is the only criterion for determining the spatial extent of "damage". In fact, the primary concern ought to be with potential permeability changes and creation of new pathways for groundwater flow.
- p. I.3 The uniaxial compressive strength (UCS) value of 334 MPa (48,000 psi) for intact basalt seems rather high. A mean UCS value of 290 MPa for the dense interior in Cohasset is given in the table on p. I.9. Even that appears high because the data only include dense interior specimens and because the specimens that are successfully fabricated tend to be a biased sample.
- p. I.9 Although the table on this page shows a dense interior UCS value of 290.3 MPa, the rock mass vesicular UCS is estimated using  $\sigma_c = 333.6$  MPa instead of 290.3 MPa. The origin of the 333.6 MPa value is unclear and not referenced.
- The computed rock mass (vesicular) UCS of 188 MPa is higher than the given intact laboratory strength of 164 MPa! Clearly, there are at least two problems here: 1) what is labelled "UCS" is really a  $\sigma_c$  value, and 2) the  $\sigma_c$  value used for the dense interior is too high as explained in an earlier comment. Note that these strength values are used throughout the document in subsequent analyses.
- p. I.17 In using the GRC approach, the assumption of a circular opening cross-section will not, in general, result in conservative answers. This is evidenced by the results presented in Table 7 on p. I.57 of the document. For example, the depth of failed zone in the floor of a circular opening (2m radius) in the dense interior of Cohasset is 12 cm as compared to 59 cm for the placement room geometry case.
- p. I.20 A peak stress value of 90 MPa is justified as being the combination of in-situ horizontal stress and thermally-induced stress. If 61.5 MPa is accepted as the maximum in-situ horizontal stress, a thermal

stress contribution of 28.5 MPa is obtained. We assert that this value for maximum thermal stress is too low. Two formulae can be used to estimate thermal stresses due to a given temperature change  $\Delta T$ . If unrestrained in one direction,  $\Delta\sigma$  in that direction is given by  $E\alpha\Delta T/(1-\nu)$ ; if restrained,  $\Delta\sigma$  is given by  $E\alpha\Delta T/(1-2\nu)$ . Let  $E = 38 \text{ GPa}$ ,  $\alpha = 6 \times 10^{-6}/^{\circ}\text{C}$ ,  $\nu = 0.25$ , and  $\Delta T_{\text{max}} = 152 \text{ }^{\circ}\text{C}$  (assuming a rock temperature of  $204 \text{ }^{\circ}\text{C}$  near canister and an ambient temperature of  $52 \text{ }^{\circ}\text{C}$ , p. II.2 and p. I.2). Substitution into the above formulae gives  $\Delta\sigma$  values of 46 MPa and 69 MPa, respectively. These higher thermal stress values, in concert with a more realistic (i.e., lower) strength value are certain to enlarge the extent of damaged rock zone.

The empirical equation  $\sigma_{\theta} = (2.01 K - 0.966) \sigma_y$  is good only for the particular geometry analyzed in "Engineering Study No. 9" (RKE/PB 1985, pp. 324-330). It is unclear as to what is meant by "optimum canister spacing".

- p. I.21 In Table 3,  $\sigma_h = 90 \text{ MPa}$  implies a  $\Delta T$  value of  $94 \text{ }^{\circ}\text{C}$  if  $\Delta\sigma = E\alpha\Delta T/(1-\nu)$  is utilized. This may or may not be representative of the worst case.
- p. I.22 The use of  $\Delta\sigma = E\alpha\Delta T$  is questionable. The formulae given above are thought to be more appropriate for estimating thermal stresses.
- p. I.64 The maximum thermally-induced stress is stated as being approximately 30 MPa. We used an analytical solution to estimate the maximum thermal stress due to a peak temperature change (i.e.,  $\Delta T_{\text{max}}$ ) of  $152 \text{ }^{\circ}\text{C}$  at the emplacement hole. A steady-state temperature distribution for a hollow cylinder was used with no temperature change at or beyond a 25 m and 50 m. The thermal stress was found to be 46 MPa. Computer printout is attached that shows the stress level to be roughly 46 MPa for two locations of zero temperature change boundary: at 25 m and at 50 m. All other input data were the same as in the document.
- p. II.2 The temperature and rates of temperature change (maximum gradients) given on this page are for a canister pitch of 22 ft. For a lower pitch, these values will increase. This needs to be emphasized. The selection of a year as the unit of time could mask transients that happen on a shorter time scale.
- p. II.4 Again, the choice of volume change per year is arbitrary. Why not use the maximum temperature change to determine the volume change regardless of time?
- p. II.6 The computed pressure change near the canister is given as 386 psi (or 272 m head). It would seem that such change is a significant perturbation on pore pressure.
- p. II.8 The vesicle pressure of 13.6 MPa due to thermal expansion is in addition to the ambient pore pressure of 9.4 MPa. When added, it gives a total pore pressure of 23 MPa, not much lower than the

fracture stress value of 24 to 29 MPa. In fact, if the range of in-situ tensile strength data presented in Table 1 is considered, the pressure change required to cause fracturing ranges from 14.2 MPa to 35 MPa for the dense interior basalt. Therefore, we disagree with the assertion that fracture could not be caused.

- p. II.9 The back-calculation to obtain a vesicle radius is confusing. Should not that be a given or measured quantity?
- p. II.10 The statement that, "... more fluid than the amounts shown will flow out of the vesicles due to the decrease in fluid viscosity at elevated temperatures." inherently assumes that the pores are interconnected. Of course, such interconnections could develop due to fracture initiation (that the author claims will not occur).
- p. II.11 The point raised in the previous review comment regarding fracture initiation and subsequent interconnections is indeed supported by the conclusion in the final paragraph.

## ATTACHMENT IB

Subject: Independent Analysis and Verification of Thermomechanical Stress Calculations Presented in the BWIP Computational Brief

### Introduction

Three different Ground Reaction Curve (GRC) methods and the VISCOT model were used by S. J. Mitchell to analyze the extent of the damaged rock zone for BWIP excavations. A review of the "Computational Brief" in which Mitchell has reported his analysis and results suggests that the stresses and the extent of the damaged rock zone may have been underestimated. Some independent analyses have been carried out with simple techniques and computer programs developed for the NRC at SNLA. The analyses and results are presented below.

### Analysis and Results

Analytical and numerical solutions of stress distribution around excavations subjected to formation stresses and/or thermal loads have been used to verify (or contradict) Mitchell's results. Circular openings in dense interior basalt and vesicular basalt have been considered. In addition, an emplacement room geometry in the dense interior has been analyzed.

The thermal and mechanical material properties used are the same as those used by Mitchell. The material property data are summarized for reference:

	<u>Dense Interior</u>	<u>Vesicular Zone</u>
Young's Modulus, E (GPa)	38.0	26.0
Poisson's Ratio, $\nu$	0.25	0.29
Unconfined Compressive Strength or UCS, $\sigma_c$ (MPa)	333.6	188.0
Hoek-Brown Parameters:		
m	18.44	10.0
s	0.0375	0.0375
Coefficient of thermal expansion (/°C)	$6 \times 10^{-6}$	$6 \times 10^{-6}$

Rather than applying a uniform stress increase everywhere due to a constant temperature increase, the present analysis uses a steady-state temperature distribution. This distribution is appropriate for a hollow cylinder of arbitrary thickness and simulates the emplacement hole geometry. By prescribing a peak temperature at the inner surface of the hollow cylinder, a spatial distribution of temperature and stress can be calculated with THCYLB1; the stresses thus calculated are the thermal stresses. The baseline boundary stresses are:

$$\begin{aligned} \text{Vertical overburden, } \sigma_v &= 24.2 \text{ MPa} \\ \text{Maximum horizontal stress, } \sigma_{h_1} &= 61.5 \text{ MPa} \end{aligned}$$

Minimum horizontal stress  $\sigma_{h_2} = 33.8$  MPa

(see p. I.20, S. J. Mitchell, 1986)

Several sensitivity cases were analyzed. Using the boundary element code CAVITY, variations of boundary stresses and basalt type were defined and solutions obtained for a circular opening of 2 m radius. Two cases of the emplacement room geometry were also analyzed; one in greater detail by using CAVITY for the drift geometry, and EXCAV2 and THCYLB1 for the circular emplacement hole. Superposition of local stresses calculated by CAVITY, EXCAV2, and THCYLB1 gives the peak thermomechanical stresses experienced in the emplacement hole wall. A definition of the different cases is given in Table 1. The Hoek-Brown failure criterion is used in every simulation with CAVITY. Cases 1 through 4 correspond to a subset of all the cases considered by Mitchell. Case 5 considers loading combinations that are thought to be more realistic, but were not considered by Mitchell. The first four cases do not explicitly account for thermal stresses and do not include the effect of excavating an emplacement hole. The predicted radial displacement and depth of failed zone are compared in Tables 2 and 3 for the first four cases.

An examination of Tables 2 and 3 shows good qualitative agreement between the results of the two sets of analyses with respect to displacement and depth of failed zone. However, a major point of contention is the selection of boundary loads for the emplacement hole. In our opinion, it is necessary to conduct appropriate analyses that take into account the excavation stresses due to both the drift and the emplacement hole. Further, thermal stresses for a non-uniform temperature distribution should result in larger total stress at the hole wall than that predicted by Mitchell. In principle, a complex three-dimensional analysis could be carried out that considers the intersection of drift and emplacement hole as well as a realistic temperature distribution. But such calculations are inefficient and expensive. An alternate approach is used here that consists of three separate (but not totally independent) solutions in two dimensions. The steps are: 1) compute the stress field around a drift of a given geometry, 2) select a peak stress value from the first solution consistent with the location and orientation of the waste package emplacement hole, 3) compute stress field around the emplacement hole using "modified" in-situ stresses (i.e., one of the new in-situ stress values is from Step 2), 4) compute thermal stress for an assumed temperature field around a circular hole, and 5) superimpose stresses from Steps 3 and 4 to obtain thermomechanical stresses in the vicinity of the hole.

Following the steps given above, Case 5 was analyzed in which the emplacement room geometry of Case 4 was subjected to in-situ stresses of 61.5 MPa (horizontal) and 24.2 MPa (vertical) and solved with CAVITY. A modified vertical stress value of 52 MPa (from the CAVITY results) and a horizontal stress value of 33 MPa were applied as boundary stresses for a circular opening of 0.813 m radius. The peak stress (not including thermal stress) in the hole wall is predicted to be 122 MPa. In a separate calculation, thermal stresses around a circular hole of radius 0.813 m are computed with THCYLB1. The imposed temperature field is appropriate for a thick hollow cylinder. The assumed temperature increase at the hole wall is 152 °C and the outer boundary for zero temperature change is arbitrarily selected at 25 m. The maximum tangential stress in the hole wall due to the

thermal load is computed to be 27 MPa. When added to the peak mechanical stress of 122 MPa, a thermomechanical stress of 149 MPa is obtained. Note that the longitudinal thermal stress is 40 MPa which must be added to the in-situ stress of at least 61.5 MPa. All of these stress values are significantly higher than the ones suggested by Mitchell. Given the uncertainty in the strength data and omission of aggravating factors such as superposition of excavation stresses and thermal gradients, we submit that the extent of the failure zone is very likely underestimated in the analysis presented by Mitchell.

Case #	Drift Geometry	Basalt Type	Initial in-situ or Boundary Stresses		Failure Criterion
			vertical	horizontal	
1	Circular 2 m radius	Dense interior	61.5	61.5	Hoek-Brown
2	Circular 2 m radius	Dense interior	24.2	90.0	Hoek-Brown
3	Circular 2 m radius	Vesicular zone	24.2	90.0	Hoek-Brown
4	Emplacement room config.	Dense interior	24.2	90.0	Hoek-Brown
5	Emplacement room config.	Dense interior	24.2	61.5	Hoek-Brown

Table 1. Sensitivity Runs with Boundary Element Computer Code

Case #	Mitchell's Analysis			Present Analysis
	GRC1 cm	GRC2 cm	GRC3 cm	cm
1	0.46	1.11	0.43	0.42
2	-	-	R = F = 0.14 S = 0.83	R = F = 0.06 S = 0.83
3	-	-	R = F = 1.22 S = 1.34	R = F = 0.04 S = 1.20
4	VISCOT	R = 0.37 F = 0.26 S = 0.71		R = 0.12 F = 0.27 S = 0.70

Table 2. Comparison of Radial Displacements in Hypothetical BWIP Openings

Case #	Mitchell's Analysis			Present Analysis cm
	GRC1 cm	GRC2 cm	GRC3 cm	
1	9.48	4.20	2.20	> 4.0; < 6.0
2	-	-	R = F = 10.96 S = 0.0	R = F = 9.0 S > 25.0
3	-	-	R = F = 36.05 S = 0.0	R, F > 20.0* S > 20.0*
4	VISCOT	R = 21.0 F = 59.0 S = 33.0		R = 17.0 25 < F < 50 25 < S < 50

\*Even though the roof, floor, and mid-pillar indicate failure depths that are less than 30 cm, other locations in the walls show failed zone depths of upto 90 cm.

Table 3. Comparison of Failed Zone Depths in Hypothetical BWIP Openings

## ATTACHMENT II

### STEALTH 2D MODEL OF BWIP EXPLORATORY SHAFT

Two-dimensional numerical model calculations have been performed to analyze the stress field around a shaft at the BWIP site. A horizontal cross-section is considered as shown in Figure 1. The computational mesh for the analysis is shown in Figure 2. A finished inside diameter of 1.83 m (6 ft) and a liner thickness of 3.5 cm (1.375 in) were defined. A cement grout thickness of about 42 cm (1.4 ft) was assumed behind the liner. The mechanical property data selected as input are given in Table 1. The initial in-situ stresses and boundary stresses are  $\sigma_{h_2} = \sigma_x = 33$  MPa and  $\sigma_{h_1} = \sigma_y = 61.5$  MPa. In Figure 2, the right and top boundaries are constant pressure (i.e., stress) boundaries with  $\sigma_{h_1}$  on right and  $\sigma_{h_2}$  on top. The left and bottom boundaries are roller (i.e., zero normal displacement) boundaries to simulate planes of symmetry; for the applied external loads it is sufficient to consider a 90° sector of the shaft cross-section. A listing of the STEALTH input data is included as Table 2; this data set supersedes an earlier one attached with the October 1986 monthly report. After some trial and error runs, two final computer runs were made. Run 1 considers the entire simulation region as basalt with a 6 ft diameter hole. The results of that run serve two purposes- 1) provide a benchmark for comparison to an analytical solution for circular hole in a medium subjected to a bi-axial state of stress; and 2) give the state of stress following hole excavation, but prior to the placement of the liner and grout. The second run (Run 2) considers the steel liner, the grout, and the surrounding basalt. The results of the second run give appropriate stress distributions in the liner, grout, and adjacent rock.

An analytical solution for the case of a 6 ft hole in basalt, subjected to  $\sigma_{h_1}$  and  $\sigma_{h_2}$  as boundary stresses, was obtained with EXCAV2. Principal stresses were monitored at selected radial and azimuthal locations to compare with the corresponding STEALTH 2D solution. A comparison is made in Table 3 of analytical and numerical results for principal stresses and at four radial locations and three different angles for each radial location. The comparison is excellent and provides confidence that reliable results will be produced in Run 2 for which an analytical solution is not readily available.

The results of Run 2 are highlighted in Table 4. Assuming that the Tresca yield criterion is adequate and the yield strength values used are representative, plastic yielding failure is predicted in portions of the liner and the grout. The parameter F is defined as  $(\sigma_1 - \sigma_2)/Y$  and may be thought of as a factor of safety. It represents the proximity of the state of stress to the yield surface. Theoretically, F cannot become less than unity. This is because upon yielding the stresses are adjusted by a flow rule such that the ratio F becomes unity. Notice in Table 4 that the F value in basalt for the undisturbed (ambient) state of stress is 5.4. The rock adjacent to the grout develops stresses that correspond to F values ranging from 2 to 12 depending on the azimuthal location. This also means that if the yield strength of basalt is less than half of the value shown in Table 1, local yielding may be expected in the host rock. The liner appears

to fail plastically over a 35° sector of the 90° sector that is modeled. When symmetry is taken into account, three similar 35° regions would show failure in each of the three 90° sectors. Failure is also indicated in a 45-50° sector of the 90° sector of the grout region; i.e., half of the grout develops sufficient stress to cause it to yield according to the Tresca criterion for the given yield strength. In Figure 3, those areas of the liner and grout that are predicted to fail are identified by the cross-hatch lines. A stress tensor plot for the entire modeled region is shown in Figure 4. Despite the poor quality of the plot, a rotation of the principal stresses and the stress concentrations near the hole are evident. The variation of maximum principal stress with angle in the liner is shown in Figure 5. The maximum principal stress variation with angle in the basalt adjacent to the grout is shown in Figure 6. For the given circular shaft geometry, obvious remedies for avoiding failure are a thicker and/or higher strength liner and grout with higher yield strength (if the yielding of grout is undesirable).

The STEALTH model used in these calculations is also capable of including thermal loads, different yield/failure criteria, and other nonlinearities in the material behavior. A two-dimensional vertical cross-section of the shaft, in axial symmetry, would permit stress variations and stratigraphic variations with depth. However, it would not be able to describe unequal horizontal boundary stresses or internal stresses. We plan to analyze the vertical cross-section case in the near future.

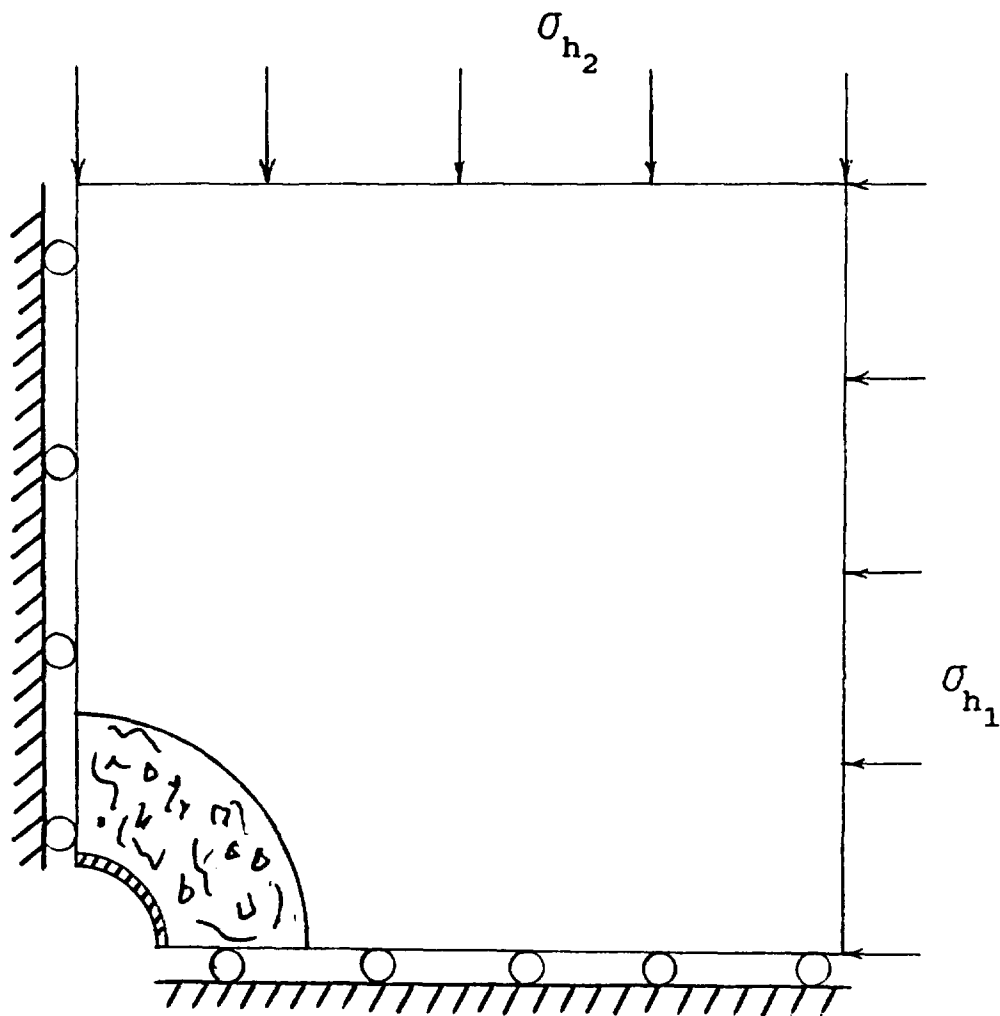


Figure 1. Two-Dimensional Model of Horizontal Cross-Section

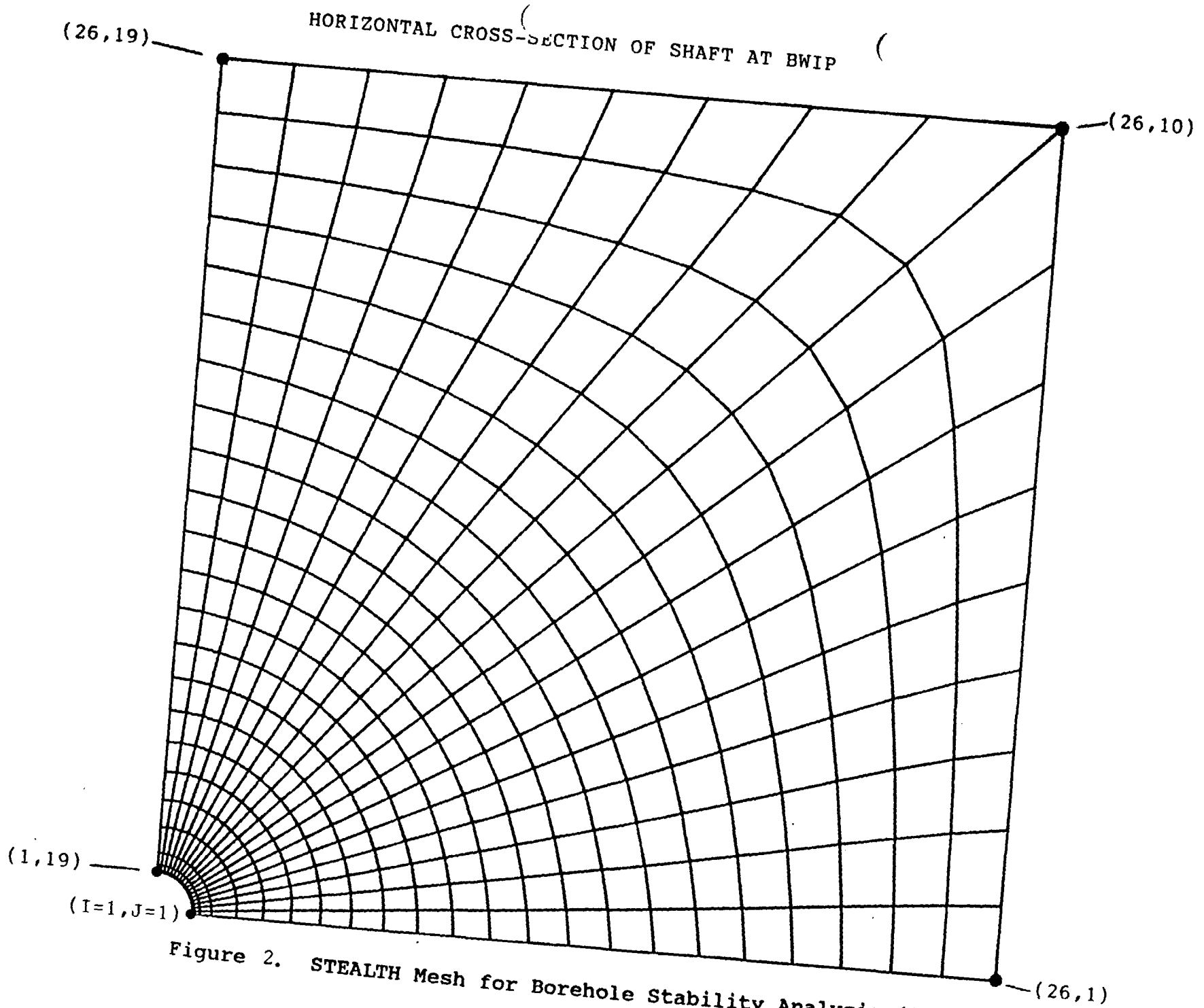


Figure 2. STEALTH Mesh for Borehole Stability Analysis (20m x 20m)

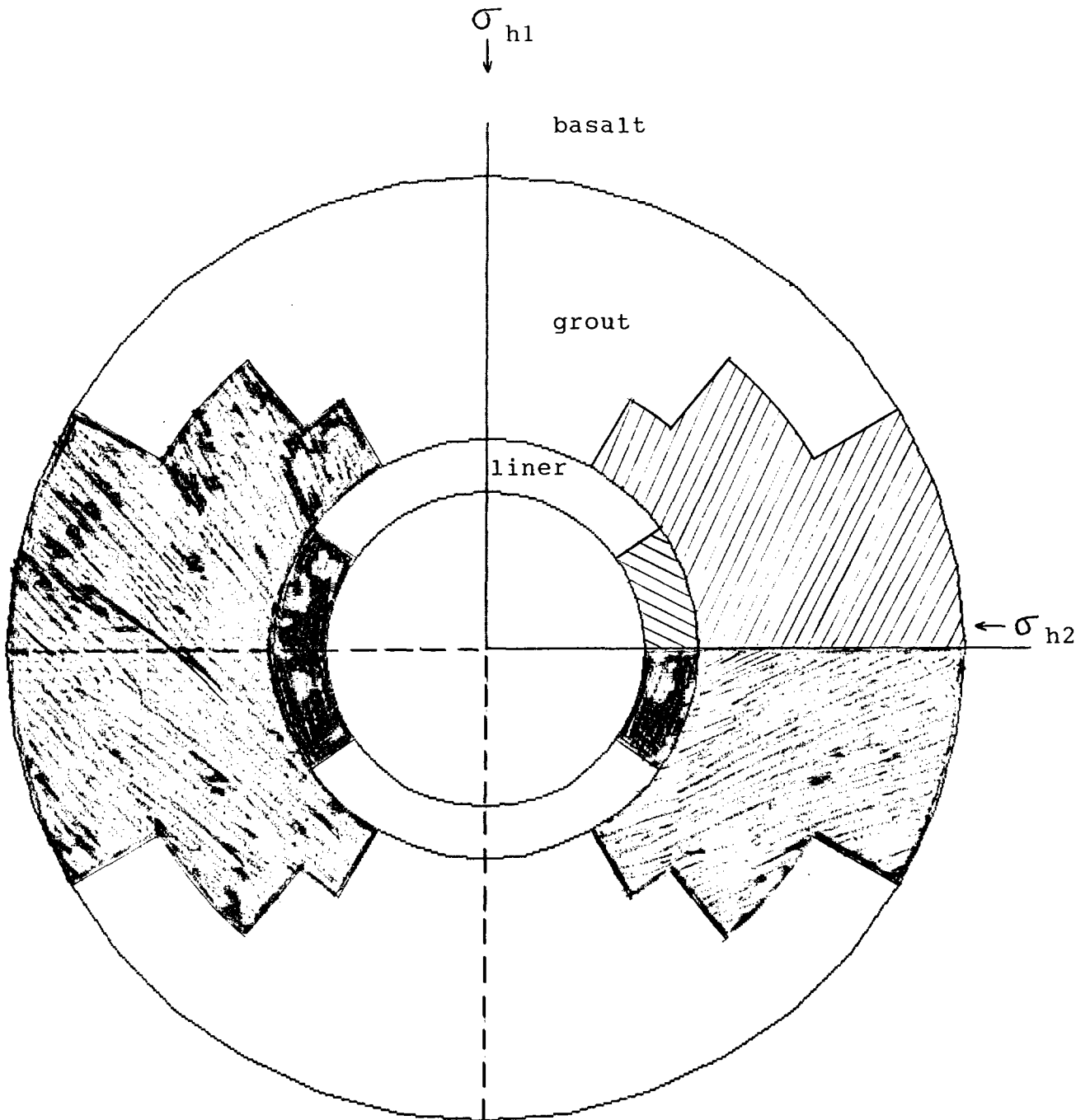
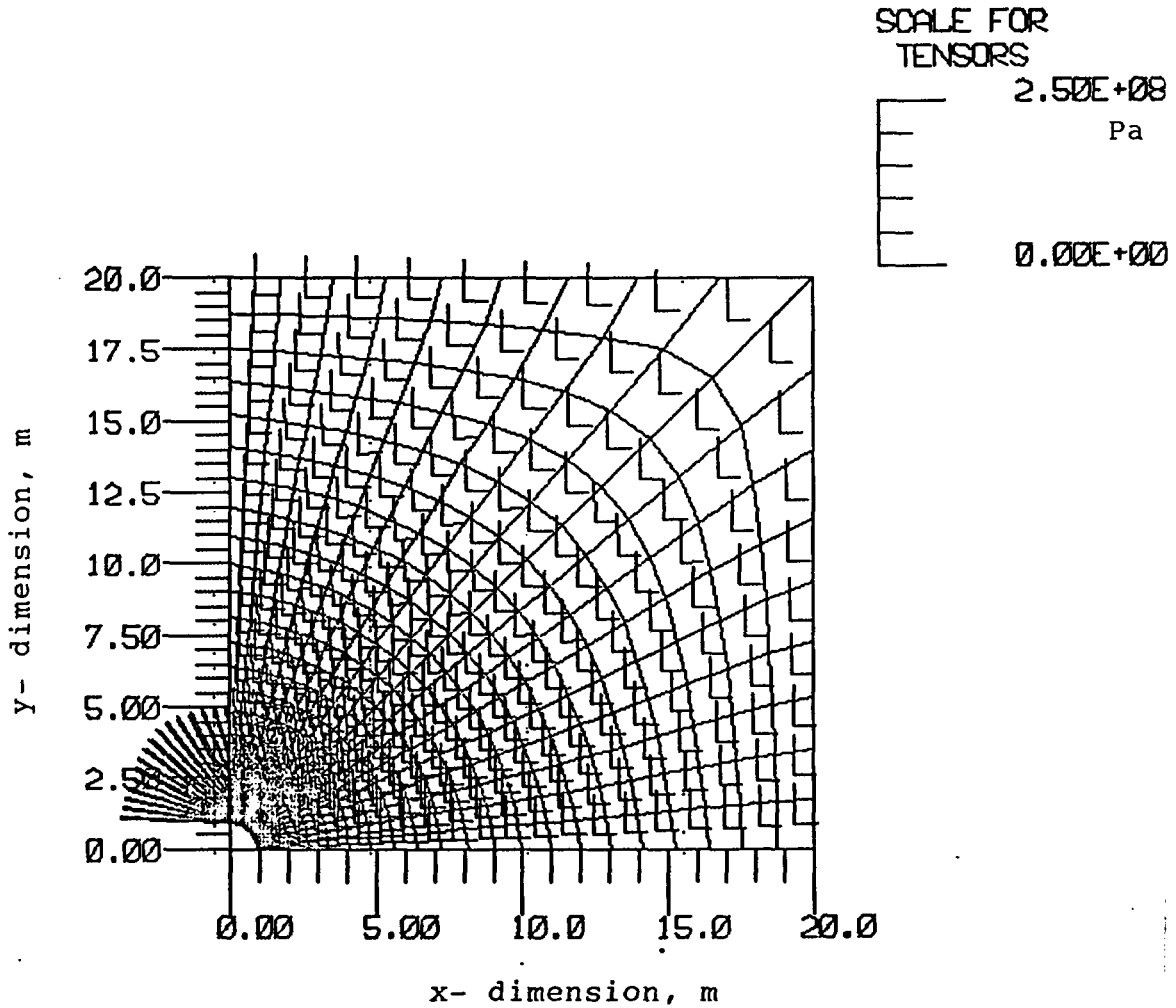


Figure 3. Plastic Yielding in steel liner and grout

\*STEALTH 2D V4-1A WI-1C12/08/86 15.18.59

BWIP HORIZONTAL X-SECTION OF SHAFT, COHASSET, W=0.25



TENSORS OF STR IN GRID NO 1  
TIME = 30.000 CYCLE = 300

Figure 4. Stress tensor plot in plane of shaft horizontal cross-section

\*STEALTH 2D V4-1A W1-1031/09/87 16:00.59

BWIP HORIZONTAL CROSS-SECTION OF SHAFT (RESTART)

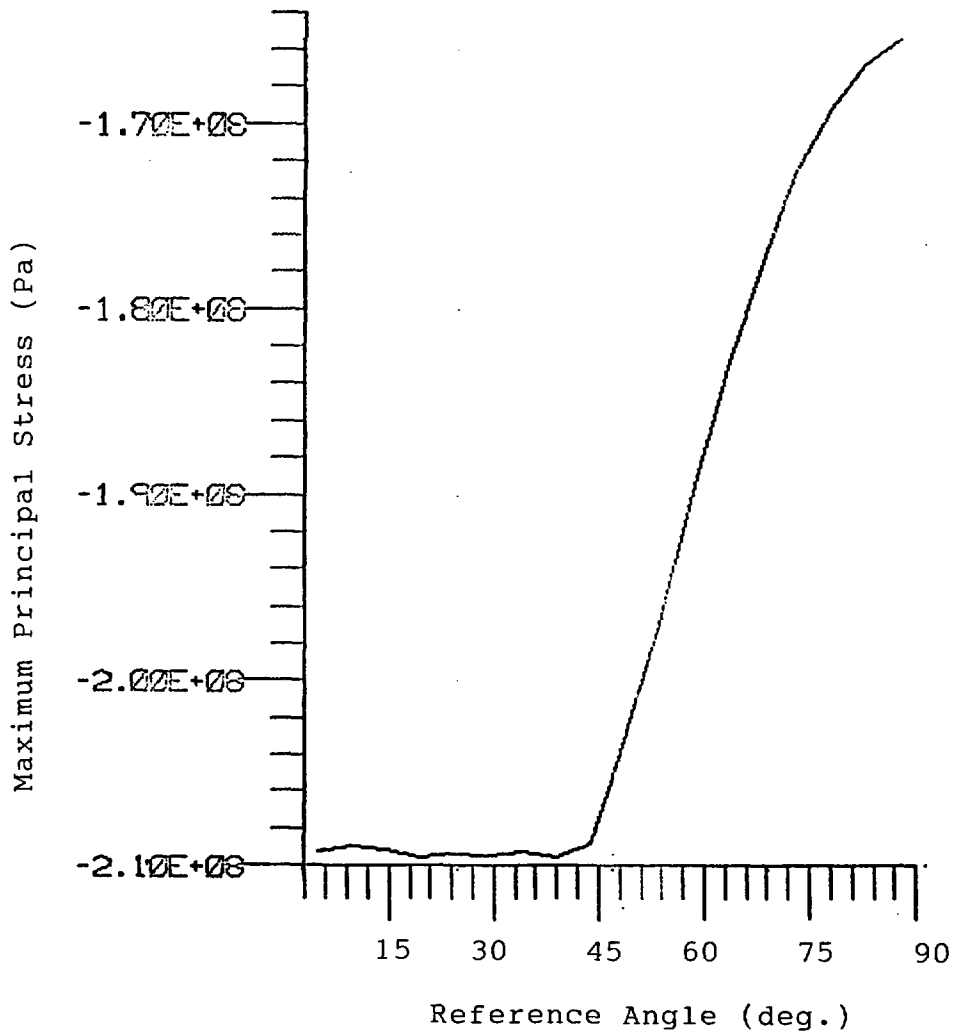


Figure 5. Variation of stress with angle in the liner

\*STEALTH 2D V4-1A WI-1001/09/87 16:00.59

BWIP HORIZONTAL CROSS-SECTION OF SHAFT (RESTART)

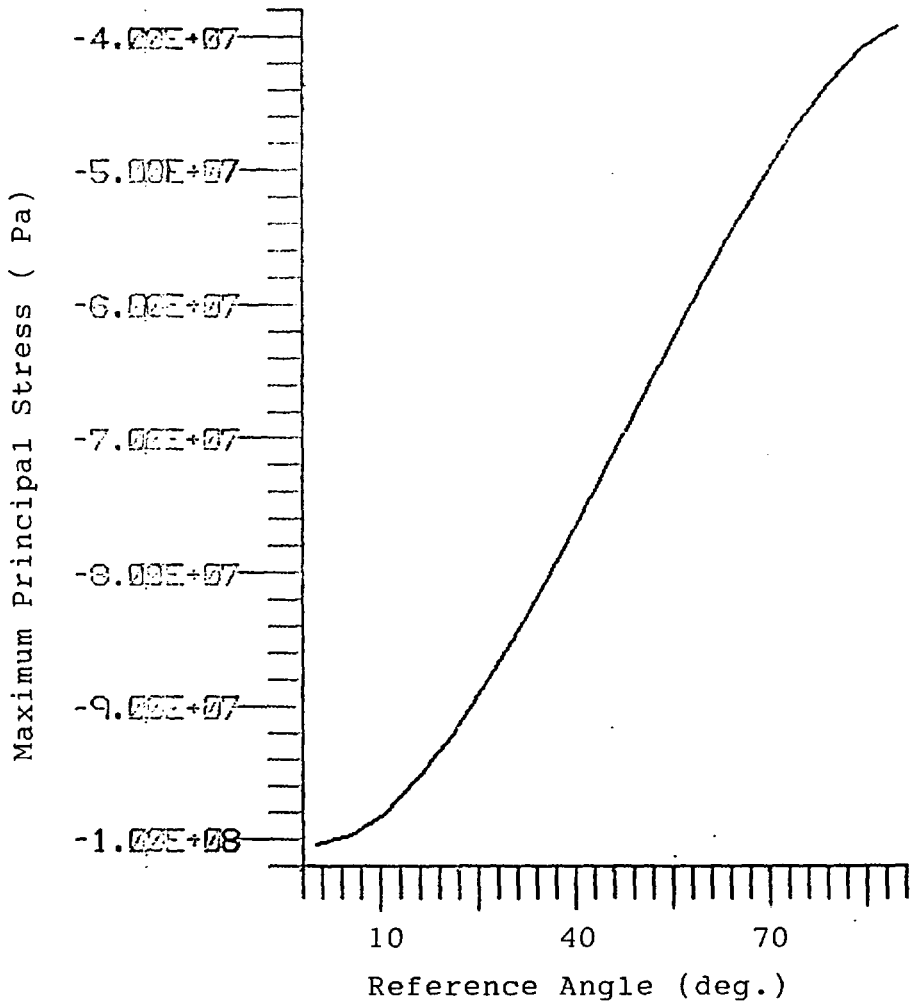


Figure 6. Variation of stress with angle in the basalt ( adjacent to grout )

BWIP 2D HORIZONTAL SHAFT CROSS-SECTION

Material	Young's Modulus E (GPa)	Poisson's Ratio $\nu$	Yield Strength Y (MPa)	Density (kg/m <sup>3</sup> )
Steel liner	196.9	0.264	207	7850
Cement grout	15.0	0.290	15	1900
Intact basalt (Cohasset)	74.4	0.250	150	2830

Table 1. Mechanical Properties of Steel Liner, Grout, and Basalt.

Table 2. STEALTH 2D Input Data

```

TTL          BWIP HORIZONTAL X-SECTION OF SHAFT, COHASSET, W=0.
PRB
PRO          2.0
DTS          2.0      1.
GRD          1.0      1.0      26.0      19.0
END
MAT
111 COHAS 1.0      1.0
112          1.0      2.0      2.0      2.0
121          1.0      2830.0
122          1.0      1.      0.      4.96 E10
132          1.0      1.50 EB
134          1.0      2.97 E10
136          1.0      -2.9 E7
111 GROUT 2.0      1.0
112          2.0      2.0      2.0      2.0
121          2.0      1900.0
122          2.0      1.      0.      1.169 E10
132          2.0      1.50 E7
134          2.0      5.83 E9
136          2.0      -1.00 E7
111 LINER 3.0      1.0
112          3.0      2.0      2.0      2.0
121          3.0      7850.0
122          3.0      1.      0.      1.390 E11
132          3.0      2.07 EB
134          3.0      7.79 E10
136          3.0      -3.45 EB
END
GPT
211          1.0      1.0      1.0      2.0      1.0
212          1.0      0.5      0.      0.914      0.
212          2.0      25.0      0.      2.0
212          3.0      0.      25.      3.0
212          4.0      0.      0.5      2.0
221          1.      1.      26.      1.      19.
283          1.
END
ZON
311 LINER 1.0      1.0      3.0      1.0      1.0
321          1.0      3.0
322          1.0      0.99988929
341          1.      -1.539 E7 -1.539 E7 -1.539 E7
311 GROUT 2.0      3.0      6.0      1.0      19.0
321          2.0      2.0
322          2.0      0.99868522
341          2.0      -1.539 E7 -1.539 E7 -1.539 E7
311 BASALT 3.0      6.0      26.0      1.0      19.0
321          3.0      1.0
322          3.0      0.99920225
341          3.0      -3.3 E7 -6.15 E7 -2.420 E7
END

```

Table 2. STEALTH 2D Input Data (cont'd)

BDY						1.0
411	BSEG1	1.0	1.0	1.0	26.0	1.0
411	BSEG2	2.0	26.0	1.0	26.0	10.0
411	BSEG3	3.0	26.0	10.0	26.0	19.0
411	BSEG4	4.0	26.0	19.0	1.0	19.0
411	BSEG5	5.0	1.0	19.0	1.0	1.0
412		1.0	1.0	6.0	5.0	2.0
412	BSEG2	2.0	1.0	2.0	5.0	1.0
412	BSEG3	3.0	1.0	2.0	5.0	3.0
412		4.0	1.0	6.0	5.0	4.0
412		5.0	1.0	3.0	5.0	
414		1.0			1.0	
414		3.0			1.0	
422	BSEG2	1.0	1.0			
431		1.0	1.0	0.0		1.0 E19
432		1.0		3.3 E7		
422	BSEG3	3.0	2.0			
431		2.0	1.0	0.0		1.0 E19
432		2.0		6.15 E7		
481		1.0	1.0	2.0		
481		4.0	3.0	4.0		
482		1.0	1.0	5.0	5.0	
482		4.0	1.0	5.0	5.0	
END						
TIM						
511		0.1				
512		0.1	0.1			
513		1.0	1.0			
514		0.25				
521		1000.0	300.			
END						
EDT						1.
611		2.0				
613		2.0				
616		2.0				
621		1.0	0.	300.0	100.0	
622		1.0	26.0	1.0	19.0	
623		11.0	14.0	71.0	72.0	73.0
623		83.	74.	64.	91.	93.
623		12.	15.			
671		1.	0.	300.	3.	
674		1.	1.	71.	1.	2002.
674		2.	1.	71.	1.	4010.
674		3.	1.	71.	1.	26019.
674		4.	1.	71.	1.	16010.
674		5.	1.	5.	1.	
675		6.	3.			300.
675		7.	6.			300.
674		8.	1.	64.	1.	21009.
674		9.	1.	72.	1.	16010.
674		10.	1.	91.	1.	10010.
END						
END						

STRESS DISTRIBUTION AROUND SHAFT BOREHOLE

$$\sigma_{h_1} = 6.15 \times 10^7$$

$$\sigma_{h_2} = 3.30 \times 10^7$$

$$r_0 = 0.914 \text{ m}$$

Radial Location $r$ (m)	Angular Location $\theta$ (deg)	Maximum Principal Stress $\sigma_1$ (MPa)		Minimum Principal Stress $\sigma_2$ (MPa)	
		Analytical	Numerical	Analytical	Numerical
0.9227	2.5	148.8	146.0	1.4	1.3
	42.5	98.5	98.4	0.9	0.9
	87.5	38.4	41.2	0.4	0.48
1.0053	2.5	129.6	128.0	11.8	10.3
	42.5	91.0	91.1	7.6	7.4
	87.5	43.0	45.0	4.5	5.8
1.6825	2.5	79.2	80.0	32.1	30.7
	42.5	71.9	71.7	24.0	24.3
	87.5	43.6	43.8	34.2	34.8
19.38	2.5	61.6	61.56	33.021	33.0
	87.5	61.27	61.49	33.104	33.5

Table 3. Comparison of Analytical and Numerical Solution Results

BWIP 2D HORIZONTAL SHAFT CROSS-SECTION

Material and Location	Maximum Principal Stress $\sigma_1$ , (MPa)	Minimum Principal Stress $\sigma_2$ , (MPa)	Proximity to Yield F $(\sigma_1 - \sigma_2)/Y$	Maximum Shear Stress $\sigma_{xy}$ , (MPa)
Liner	Range: 165-209 $\sigma_3$ : 52-187	Range: 2.0-2.7	Range: 1.00-1.27 Yielding over 35° sector	102.0
Grout	Range: 22.6-26.5 $\sigma_3$ : 17.3-64.0	Range: 9.7-16.1	Range: 1.00-5.05 Yielding over 45° sector	7.3
Basalt adjacent to grout	Range: 39.3-100.4 $\sigma_3$ : 17.2-31.4	Range: 21.7-27.1	Range: 1.9-12.4	22.3
Basalt (ambient)	61.5 $\sigma_3$ : 24.2	33.0	5.4	0

Table 4. Stress Distribution in the Liner, Grout, and Host Rock

### ATTACHMENT III

During December, the STEALTH 3D program (file FILE5ST located in user area KKWAHI) was converted to "Update" format. This was accomplished by 1) inserting the DECK directive to define decks for overlays, programs, subroutines and functions; 2) inserting the COMDECK directive to define common blocks and relocating a copy of each common block to the beginning of the file; and 3) removing subsequent explicit statements of common blocks and inserting the CALL directive.

Macros were developed to insert a total of 251 "\*DECK" directives, 25 "\*COMDECK" directives, and replace 626 explicit statements of common blocks with "\*CALL" directives. These macros are currently available in the user area GFWILKI for future use.

The Update file named BIGBOY is saved in user area GFWILKI and has been made available for public access. In addition, the file BIGBOY was run through the Update processor to create an old program library (OLDPL), the program library which can then be updated in subsequent Update runs. The OLDPL has been saved under the file name STOPL. The compile file, named STLCMP1, contains copies of decks in the program library restored to a format that can be processed by a compiler or assembler. STOPL and STLCMP1 are also public files in user area GFWILKI.

A-1755  
 1628.010  
 December 1986

THIS IS AN ESTIMATE ONLY AND MAY NOT MATCH THE INVOICES SENT TO NRC BY SANDIA'S ACCOUNTING DEPARTMENT.

	Current Month	Year -to- Date
	-----	-----
I. Direct Manpower (man-months of charged effort)	0.4	1.0
II. Direct Loaded Labor Costs	2.0	5.0
Materials and Services	0.0	0.0
ADP Support (computer)	1.0	1.0
Subcontracts	16.0	3.0
Travel	0.0	0.0
Other (computer roundoff)	-1.0	0.0
	-----	-----
TOTAL COSTS	18.0	9.0

III. Funding Status

Prior FY Carryover	FY 87 Projected Funding Level	FY 87 Funds Received to Date	FY 87 Funding Balance Needed
-----	-----	-----	-----
None	250K	250K	None